WELD IMAGE DUST REMOVAL ALGORITHM BASED ON FUSION OF BRIGHT CHANNEL AND WEIGHTED GUIDE DARK CHANNEL

Qingchun ZHENG[1,2], Kaijie LU[1,2], Wenpeng MA[1,2,*], Zhidong ZHANG[1,2], Peihao ZHU[1,2], Jingna LIU[1,2], Yahui HU[1,2]

The dust removal technology of weld image is helpful to promote the development of weld target detection and tracking control. Aiming at the problem that the image restoration algorithm has halo phenomenon in depth discontinuity and easy to cause color distortion, this paper proposes a single image restoration algorithm based on fusion of bright channel and weighted guided dark channel for dedusting of weld image. Firstly, the bright channel hypothesis is derived according to dark channel priori (DCP), and the bright channel obtained by the adaptive method will fuse with the dark channel image to construct the fusion channel. Then, the weighted guided filter is used to optimize the rough transmittance. Finally, the restored image of the weld is recovered according to the atmospheric scattering model and the restored atmospheric light. Simulation experiments and image quality analysis show that the proposed algorithm can recover the details of the weld image and suppress the halo phenomenon. The image segmentation networks are used to further verify that our algorithm can improve the accuracy and integrity of weld segmentation.

Keywords: Image restoration, DCP, Bright channel hypothesis, Weighted guided filtering, Image segmentation

1. Introduction

With the rapid advance of intelligent manufacturing industry, the complex welding seam polishing automation requires the accuracy and efficiency of identification. In the welding seam grinding and polishing workshop, the image quality obtained by the indoor welding seam image acquisition system is affected to different degrees by a large amount of dust and Mars interference [1]. Therefore, it is of great practical significance to dust removal of weld image collected in complex environment, which is helpful to promote the development of weld target detection and tracking control.

1 Tianjin Key Laboratory for Advanced Mechatronic System Design and Intelligent Control, School of Mechanical Engineering, Tianjin University of Technology, Tianjin 300384, China
2 National Demonstration Center for Experimental Mechanical and Electrical Engineering Education (Tianjin University of Technology)
*Corresponding author: Wenpeng Ma, E-mail: 506904879@qq.com

Currently, the main weld image clearer processing is divided into two categories. One of these is to improve the image enhancement method by improving the image contrast, although it significantly improves the details of the image, but cannot completely remove the dust factor in the weld image, so that the recovered image cannot correctly show the scene information and can easily distort the image. The other is the image restoration method based on the physical model, which can directly show the degradation reason of the degraded image and reversely show the image before the degraded image.

Considering that the image acquisition system cannot accurately obtain the contour information of the image, the atmospheric scattering model shows that the dust concentration is closely related to the scene contrast, thus, single image restoration has made great progress on the basis of establishing many priors and assumptions. Zhao [2] enhanced the local brightness by using the improved multi-scale Retinex, which improves the sharpness of the image, but the restored image is oversaturated in color and halo phenomenon appeared at the abrupt change of the depth of field. Fattal [3] verified the assumption that the transmittance of light propagation is not related to the local shadow on the surface of the object and used the independent component analysis to realize the image restoration. However, this algorithm is time-consuming and cannot be used in the gray image, so it is not ideal for the image without enough color information for the component analysis. Based on the analysis of a large number of outdoor degraded images, the CVPR best paper in 2009 [4] found and proposed dark channel priori (DCP), in which a certain color channel of the pixel in the non-bright region of the image has a lower pixel value. The author estimated the concentration of air mediators by using DCP, and achieved successfully the image restoration with the help of the atmospheric scattering model. In view of the obvious halo phenomenon and the serious block effect at the abrupt change of brightness, the author [5] then proposed to optimize the transmittance through guided filtering, which achieved better results and provided an optimization idea for future generations. For example, the literature [6] adopted bilateral filtering method to smooth the transmittance map and improved the processing speed. Sun [7] proposed a local atmospheric light estimation method, which improve the problem of insufficient global atmospheric light value selection in DCP. In addition, the research shows that the deep neural network can better extract fog-related features and carry out transmittance estimation. REN [8] trains the image feature information with the multi-stage neural network and improves the image quality through bilateral linear correction, but this method is not ideal for the restoration effect of a single image.

In summary, the above methods provide important ideas for the dust removal treatment of weld image. In this paper, an improved algorithm based on the fusion of light channel and weighted guided dark channel is proposed. The fusion channel is constructed by the linear fusion of the dark channel and bright channel images obtained by the adaptive method. Then, the weighted guided filter is used to calculate the local pixel variance and refine the transmittance which will be substituted into the atmospheric scattering model to recover the weld image. Finally, the restored image is transmitted to the segmentation network, which further verifies that the algorithm can improve the precision and integrity of weld segmentation

2. Dark channel priori theory

The atmospheric scattering model proposed by McCamey [9], as an image optical model considering weather and light conditions, has been widely used in computer vision and graphics. According to the fading model and the ambient light model, the atmospheric scattering model of image degradation with fog can be simplified as:

$$I(x) = J(x)t(x) + A(1 - t(x)) \tag{1}$$

where $I(x)$ is observed intensity, $J(x)$ is restored image, A is the global atmospheric light, and $t(x)$ is the medium transmission describing the portion of the light that is not scattered and reaches the camera. The first term $J(x)t(x)$ on the right hand side of Equation (1) is called direct attenuation, and the second term $A(1-t(x))$ is called airlight absorption. In addition, as a constant, $t(x)$ is negatively correlated with the concentration of air medium. When the atmosphere is homogenous, it can be expressed as:

$$t(x) = e^{-\beta d(x)} \tag{2}$$

where β is the scattering coefficient of the atmosphere. It indicates that the scene radiance is attenuated exponentially with the scene depth $d(x)$. This formula describes that the transmittance decreases exponentially with the increase of depth of field distance.

The goal of image restoration is to recover $J(x)$, A, and $t(x)$ from $I(x)$. Because of the depth of field information cannot be accurately obtained, and the distribution of air medium is not uniform, it is very difficult to obtain the medium transmission rate directly through the Equation (2).

The DCP is based on the following observation on haze-free outdoor images: in most of the non-sky patches, at least one-color channel has very low intensity at some pixels. Formally, the dark channel $J_{(x)}^{dark}$ can be expressed as:

$$J_{(x)}^{dark} = \min_{y \in \Omega(x)} \left(\min_{c \in \{r,g,b\}} (J_c(y)) \right) \approx 0 \tag{3}$$

where $J_c(x)$ represents a certain color channel of $J(x)$, c is any of the three channels of RGB. $\Omega(x)$ is a local patch centered at x.

Combined with Equation (3) and Equation (1), the transmittance can be obtained as follows:

$$t(x) = 1 - \omega \frac{I(x)}{A(x)} \tag{4}$$

where ω is an adjustment factor that controls the degree of image restoration. To retain a certain degree of authenticity, its value is 0.95.

After the estimation of A and $t(x)$, the expression of the restored image can be obtained:

$$J(x) = \frac{I(x) - A(x)}{\max(t(x), t_0)} + A \tag{5}$$

where t_0 is used to keep the denominator from going to zero.

3. Our algorithm

The pixel value of the dark channel of the image tends to a constant in the local area by using the local minimum filter. This means that when a pixel is in the edge or bright area and the phase velocity point is high, the dark channel of the point will be replaced by the minimum value, resulting in the dark channel pixel value of the point is significantly less than the actual value, therefore, [4] cannot maintain the edge characteristics of the object. In this paper, the welding seam is taken as the object (its air medium is often referred to as iron dust). In view of the fact that dark prior is prone to color deviation and halo phenomenon on the surface of the welding seam with strong reflection, a dust-removing algorithm of welding seam image combining bright channel and weighted guidance dark channel is proposed. The method flow is shown in Fig. 1.

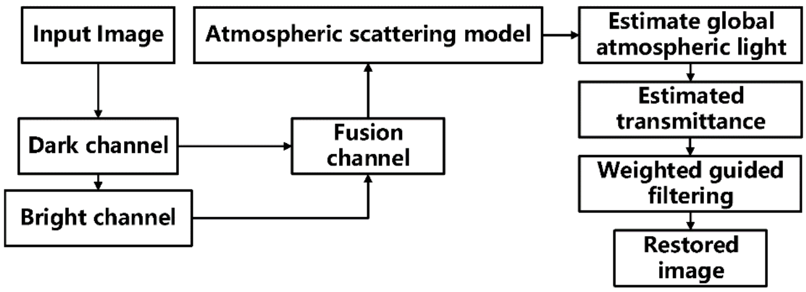

Fig.1 Flowchart of algorithm

3.1 Bright channel hypothesis

According to the definition of DCP, the bright channel hypothesis is assumed as follows: in most areas with large air media, at least one color-channel has very high intensity at some pixels. Similarly, the bright channel $J_{(x)}^{dark}$ can be expressed as:

$$J_{(x)}^{bright} = \max_{y\in\Omega(x)}(\max_{c\in\{r,g,b\}}(J_c(y))) \approx 1 \tag{6}$$

In order to achieve better effect of bright channel reconstruction, $\Omega(x)$ generally satisfies the principle of taking large neighborhood for nearby objects and small neighborhood for distant objects. Therefore, an adaptive method has chosen to normalize Equation (2), from which the size matrix of each field of the bright channel is calculated as follows:

$$\Omega'(x,y) = \frac{1}{\beta d(x,y)} = \frac{-1}{\ln(1-\frac{A^{bright'}(x)}{A^{bright}(x)})} \tag{7}$$

$$\Omega(x,y) = \alpha' \times normalize(\Omega'(x,y)) + C \tag{8}$$

where $A^{bright'}(x)$ is the adaptive atmospheric light. $\Omega'(x,y)$ is the unnormalized inverse distance matrix. α' is scale parameter and C is minimum window.

3.2 Estimate global atmospheric light

By introducing bright channel and dark channel regulators respectively, the final global atmospheric light is obtained as follows:

$$A(x) = \mu A^{bright'}(x) + \eta A^{dark}(x) \tag{9}$$

when setting the weight, the atmospheric light value obtained by following the bright channel should have a larger weight, while the atmospheric light value obtained by the dark channel should have a smaller weight and meet the conditions $\mu+\eta \le 1$. The fusion channel after synthesis is shown in Fig.2.

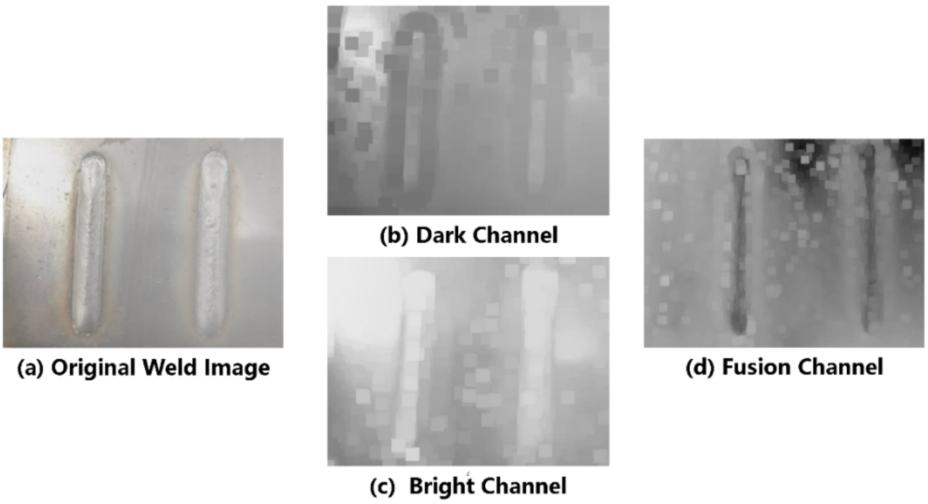

Fig.2 Fusion channel synthesis of weld image

3.3 Smooth transmittance

It can be seen from Equation (2), in a smaller local area, pixels in the same depth of field area should have similar transmittance. The weighted bootstrap filter is a local linear image filter which connects the bootstrap image with the output image. It not only has the characteristics of smoothness and edge retention, but also can adjust the parameters adaptively according to the window contents. Assuming that I is the bootstrap image and q is the output image, the filtering linear transformation model is as follows:

$$q_i = a_k I_i + b_k, \forall i \in \omega_k \tag{10}$$

where ω_k is the domain centered at pixel k, a_k and b_k are some linear coefficients assumed to be constant in ω_k. This local linear model ensures that q has an edge only if I has an edge, because $\nabla q = a \nabla I$.

According to the variance of ω_k, edge weights are defined as follows:

$$W_I(k) = \frac{1}{N} \sum_{i=1}^{N} \frac{\sigma_I^2(k) + \gamma}{\sigma_I^2(i) + \gamma} \tag{11}$$

where $\sigma_I^2(\cdot)$ represents the variance in ω_k within I, N is the total number of pixels of the bootstrap image. Specifically, we minimize the following cost function in the window:

$$E(a_k, b_k) = \sum_{i \in \omega_k} [(a_k I_i + b_k - p_i)^2 + \frac{\varepsilon}{W_1(k)} a_k^2] \tag{12}$$

Here ε is not only a regularization parameter preventing a_k from being too large, but an important parameter to adjust the filter filtering effect. Apparently, the greater the field variance of pixel k, the greater the corresponding edge weight $W_I(k)$ and the smaller the normalization factor. Therefore, weighted guided filtering can better preserve image edges.

In terms of the principle of least squares, transformation of Equation (12) is as follows:

$$\begin{cases} a_k = \dfrac{\frac{1}{|\omega|} \sum_{i \in \omega_k} I_i p_i - \mu_k \overline{p}_k}{\sigma_k^2 + \frac{\varepsilon}{W_1(k)}} \\ b_k = \overline{p}_k - a_k \mu_k \end{cases} \tag{13}$$

Here, μ_k and σ_k^2 are the mean and variable of pixels in ω_k respectively, $|\omega|$ is the number of pixels in ω_k, and $\overline{p}_k$ is the mean of p in ω_k.

After computing a_k for all patches ω_k in the image, the filter output could be computed by:

$$q_i = \overline{a}_i I_i + \overline{b}_i \tag{14}$$

where $\overline{a_i}$, $\overline{b_i}$ are the mean of a_i and b_i in ω_k, respectively. The weighted boot filter is different from the traditional boot filter, which combines the mean value and variance of the neighborhood window as the estimation value of the local window, and can adjust the parameters adaptively, so as to effectively retain the edge details of the image. As shown in Fig.3, our method has a better recovery effect, in which fusion channels supplement the local contrast and weighted guided filtering can better retain the contour information of the weld.

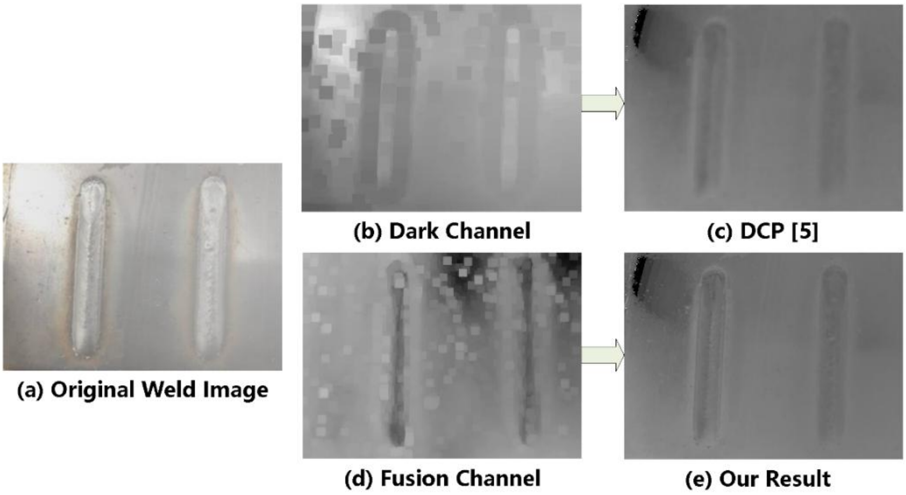

Fig.3 Transmission optimization results

4. Experiment results and analyses

In order to verify the image restoration effect, the algorithm in this paper was implemented on MATLAB, and the dust removal effect of the weld image has been compared and analyzed from subjective evaluation and objective evaluation. Finally, the image segmentation model was built using the clear weld image restored by the algorithm in this paper and the weld image containing dust as the training set, which was used to further analyze the influence of the algorithm on weld image segmentation.

4.1 Subjective evaluation

The subjective analysis can reflect the recovery effect most intuitively. In this paper, the current classical image restoration algorithm is selected for comparison. Fig. 4 shows the dust removal effect of welding seams of different algorithms. Fig. 4(a) is the original weld image. Fig. 4(b) is [2] the multi-scale Retinex based on image enhancement, it causes severe color misalignment and local contrast reduction, resulting in colors that do not look natural. Fig. 4(c) shows the dark channel prior algorithm of [5]. It basically eliminates the dust factor, but the image is obviously dark and the weld contour is not clear. In particular, Image 4 exists partial halo still. Fig. 4(d) is an image edge preserving method combining bilateral filtering with dark channel prior of [10]. Although the dust removal effect of this method is not very ideal, the brightness is moderate and the weld contour is clearly visible. Fig. 4(e) shows the recovery effect of our algorithm of which overall recovery effect is better than that the others. The bright channel hypothesis is introduced to compensate the brightness and contrast effectively, and to suppress the phenomenon of color bias and color distortion effectively. In addition, although the outline of the weld is very clear, there is still a partial halo in the highlighted area.

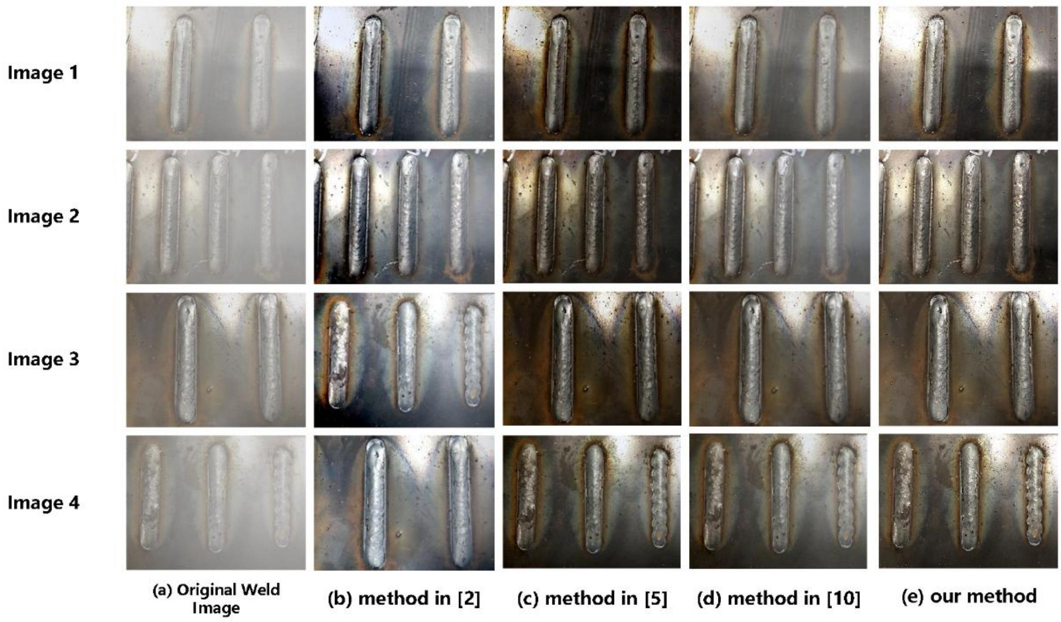

Fig.4 Contrast of weld image restoration effect

4.2 Objective evaluation

In order to further verify the effectiveness of the algorithm in this paper, the unreferenced image quality evaluation method for image enhancement effect evaluation was adopted [11], and structural similarity (SSIM), image entropy, mean gradient and mean pixel value has been selected as evaluation indexes.

Compared with other algorithms, the objective evaluation analysis of the four graphs from Fig.4 processed by these algorithms is shown in the Fig.5. Obviously, our method has achieved a good performance that the score of similarity with the original figure is above 0.85 from Fig. 5(a). It can be seen from Fig. 5(b) that the average information amount of the above methods is not much different, indicating that weighted guided filtering can also effectively refine the transmittance and solve the block effect to some extent. Fig. 5(c) shows that our method and [2] are obviously superior to other methods in the effect of weld edge transition. In addition, our method uses bright channel to compensate the brightness loss, which greatly improves the contrast and brightness compared with other methods. Therefore, it can be seen in Fig. 5(d) that the mean pixel value performs better.

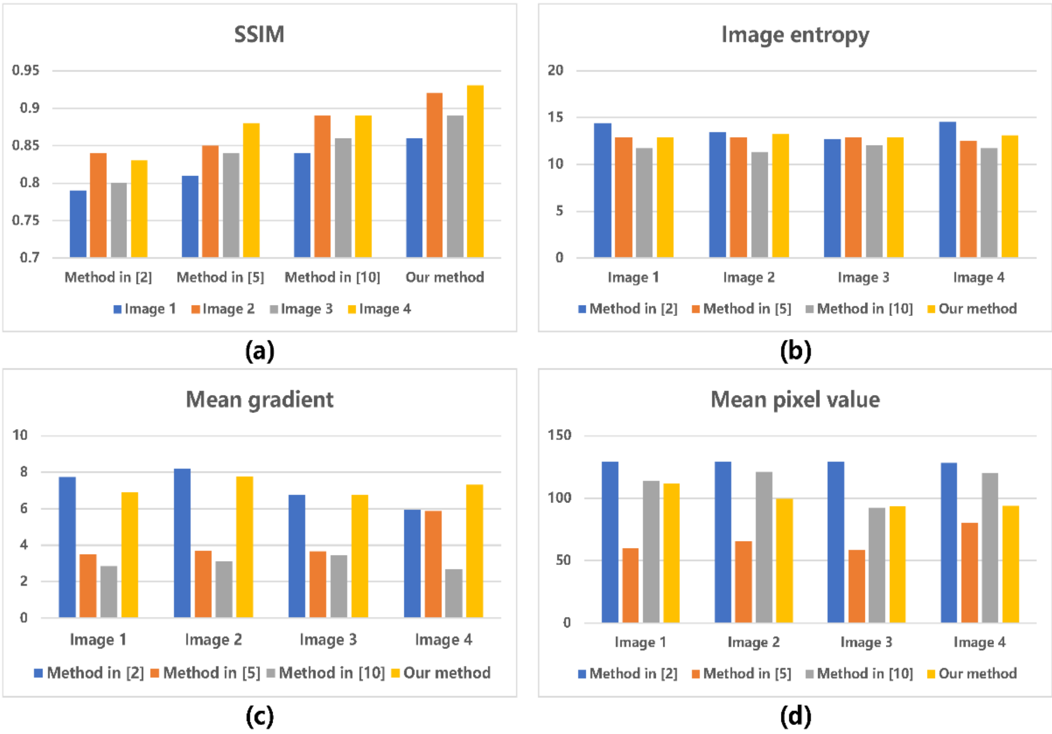

Fig.5 Objective evaluation

4.3 Image segmentation

In this experiment, PyTorch1.5 was used as the deep learning framework to build the development environment, and two classical segmentation networks were selected for the experiment. Among them, Mask R-CNN [12] was realized with the help of MMDetection2.0 [13], an open source object detection toolbox developed by Multimedia Laboratory, CUHK. Another one is the segmentation network YOLACT++ [14] with higher speed and lower accuracy.

The original image data set of weld containing dust and the image data set of weld restored by the algorithm were expanded to 320 by random scaling and random rotation. During the training, Resnet pre-training model was used to initialize parameters, the epochs were set the same training cycle in GPU acceleration mode. The segmentation model after consistent tuning was used to detect multiple groups of images, and the detection results are shown in Fig. 6 and Fig. 7.

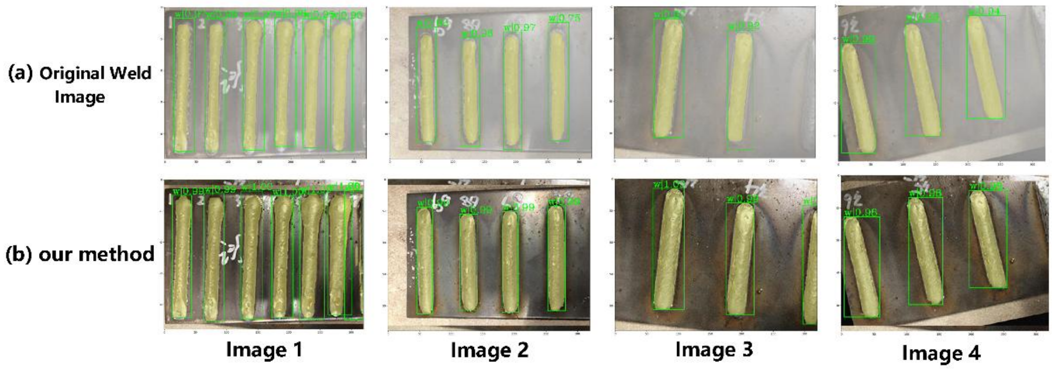

Fig.6 Experimental results of Mask R-CNN segmented network

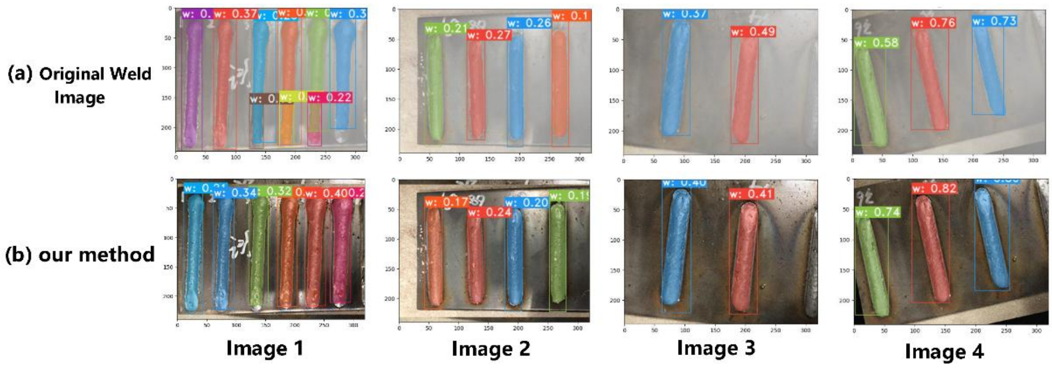

Fig.7 Experimental results of Yolact++ segmented network

Obviously, it can be seen from Fig. 6 that the model generated without image restoration has a relatively low accuracy rate and cannot be completely segmented, especially the serious loss of information about the edge of some welding seams. On the contrary, the weld image processed by the image restoration algorithm in this paper can effectively improve the precision of the segmentation model, and the average accuracy can reach more than 0.9, and the weld can be segmented completely. In addition, it can be seen from Fig. 7 that in the network with low relative accuracy, there is no significant difference in the segmentation accuracy between the two. However, after processing with our method, the integrity of weld segmentation in Image1 is slightly improved.

5. Conclusions

Aiming at the problem that the transmittance estimation of DCP is not accurate at the sudden change of depth of field and the contrast drops significantly, this paper proposed an image restoration algorithm based on combining the bright channel and dark channel for dedusting weld image, and the weighted guided filter is used to obtain a more accurate and delicate transmittance map. Experimental results show that the image reconstructed by our method has higher color fidelity, better contrast, more details, and can improve the integrity of weld segmentation and the precision of the segmentation model in the practical application of image segmentation. In addition, the follow-up work can improve the accuracy of transmittance estimation and alleviate the problem of color supersaturation by proposing a new adaptive fusion method for high-quality fusion channels.

Acknowledgement

The work is supported by the Tianjin Science and Technology Project (Grant No.19YFFCYS00110), the National Natural Science Foundation of China (Grant No. 61941305), the Natural Science Foundation of Tianjin of China (Grant No.18JCQNJC75000), and the Belt and Road International Scientific and Technological Cooperation Demonstration Project (Grant No. 17PTYPHZ20060).

R E F E R E N C E S

[1]. *R. Ranjan, A. R. khan, C. Parikh, et al,* "Classification and identification of surface defects in friction stir welding: An image processing approach", in Journal of Manufacturing Processes, vol. 22, Apri. 2016, pp. 237-253.

[2]. *C. L. Zhao, J. W. Dong,* "Image enhancement algorithm of haze weather based on dark channel and multi-scale Retinex", in Laser Journal, vol. 39, no. 1, Jan. 2018, pp. 104-109.

[3]. *R. Fattal,* "Acm Transactions on Graphics", in Acm Transactions on Graphics, vol. 27, no. 3, Aug. 2008, pp.1-9.

[4]. *K. M. He, J. Sun, X. O. Tang,* "Single Image Haze Removal Using Dark Channel Prior", in 2009 IEEE Conference on Computer Vision and Pattern Recognition (CVPR), Florida, America, 2009.

[5]. *K. M. He, J. Sun, X. O. Tang,* "Guided image filtering", in IEEE Transactions on Pattern Analysisand Machine Intelligence, vol. 35, no. 6, Jun. 2013, pp. 1397-1409.

[6]. *C. Y. Pang, X. Q. Ji, L. N. Sun, et al,* "An Improved Method of Image Fast Defogging", in Acta Photonica Sinica, vol. 42, no. 7, Jul. 2013, pp, 872-877.

[7]. *W. Sun, D. J. Li, H. J. Liu, et al,* "Fast single image fog removal based on atmospheric scattering model", Guangxue Jingmi Gongcheng/optics & Precision Engineering, vol. 21, no. 4, Apr. 2013, 21(4):1040-1046.

[8]. *W. Q. Ren, S. Liu, H. Zhang, et al,* "Single Image Dehazing via Multi-scale Convolutional Neural Networks", in European Conference on Computer Vision (ECCV), Amsterdam, Netherlands, 2016.

[9]. *E. J. McCartney,* "Optics of the Atmosphere: Scattering by Molecules and Particles", in Physics Today, vol. 30, no. 5, May. 1977, pp. 76-77.
[10]. *J. X. Zeng, Y. L. Yu,* "Image defogging and edge preserving algorithm based on dark channel prior and bilateral filtering", in Journal of Image and graphics, vol. 22, no. 2, Jan. 2017, pp. 147-153.
[11]. *J. Yu, D. B. Xu, Q. M. Liao,* "Image defogging: a survey", in Journal of Image and graphics, vol. 16, no. 9, Sept. 2011, pp. 1561-1576.
[12]. *K. M. He, G. Gkioxari, D. Piotr, et al,* "Mask R-CNN", in 2017 IEEE Conference on Computer Vision and Pattern Recognition (CVPR), Hawaii, America, 2017.
[13]. *K. Chen, J. Q. Wang, J. M. Pang,* "MMDetection: Open MMLab Detection Toolbox and Benchmark", in 2019 IEEE Conference on Computer Vision and Pattern Recognition (CVPR), Los Angeles, America, 2019.
[14]. *D. Bolya, C. Zhou, F. Y. Xiao, et al,* " YOLACT++ Better Real-time Instance Segmentation" in 2019 IEEE Conference on Computer Vision and Pattern Recognition (CVPR), Los Angeles, America, 2019.